^{116}Cd(^{31}P,p5nγ) 2016Ra33

Type	Author	History Citation	Literature Cutoff Date
Full Evaluation	N. Nica	NDS 187,1 (2023)	12-Oct-2022

2016Ra33 compiled for XUNDL by B. Singh (McMaster).

2016Ra33: E(^{31}P)=148 MeV. Measured Eγ, Iγ, $\gamma\gamma$-coin, $\gamma(\theta)$, $\gamma\gamma(\theta)$(DCO), $\gamma\gamma(\theta)$(ADO), $\gamma\gamma$(linear polarization), level lifetimes by DSAM using the INGA array of 19 Compton-suppressed clover HPGe detectors arranged at six different angles at TIFR Pelletron Linac facility. Deduced high-spin levels, J^π, B(M1), magnetic-dipole rotational band. Contour plots of TRS calculations for the two bands. Comparison with principal axis cranking (SPAC) model calculation involving shears mechanism.

^{141}Sm Levels

E(level)[†‡]	J$^\pi$[‡]	T$_{1/2}$[#]	Comments
0.0[@]	1/2$^+$[@]		
1.58[@] *4*	3/2$^+$[@]		
175.8[@] *3*	11/2$^-$[@]	22.6 min *2*	%ε+%β^+=99.69 *3*; %IT=0.31 *3* T$_{1/2}$ and decay mode from Adopted Levels.
810.6[@] *5*	15/2$^-$[@]		
1899.4[@] *6*	(19/2$^-$)[@]		
2418.6[@] *6*	(23/2$^-$)[@]		
2641.1[@] *6*	(23/2$^+$)[@]		
2722.4[@] *6*	(21/2$^+$)[@]		
2822.7[@] *6*	(23/2$^+$)[@]		
3317.8[@] *6*	(23/2$^-$)[@]		
3376.4[&] *6*	25/2$^-$		
3509.0[&] *7*	27/2$^-$	1.64 ps *+31−27*	
3818.4[&] *7*	29/2$^-$	0.73 ps *+15−13*	
4264.8[&] *7*	31/2$^-$	0.50 ps *+10−9*	
4792.6[&] *7*	33/2$^-$	0.77 ps *+16−10*	
5322.7 *7*	35/2$^-$		
5340.6[a] *7*	35/2$^-$	0.28 ps *6*	
5365.6[&] *7*	(35/2$^-$)		
5594.3[a] *7*	37/2$^-$	1.30 ps *+28−24*	
5640.9 *7*	37/2$^-$		
5940.0[a] *7*	39/2$^-$	<0.80 ps	T$_{1/2}$: from effective half-life from 345.5γ, assuming 100% side feeding.
6413.0[a] *8*	41/2$^{(-)}$		
6894.4[a] *8*	43/2$^{(-)}$		
7384.4[a] *9*	45/2$^{(-)}$		

† From least-squares fit to Eγ data, assuming 0.3 keV uncertainty when not stated.

‡ From 2016Ra33 for levels above 3320 keV.

\# From 2016Ra33 by DSAM, except where noted.

@ From Adopted Levels, not detected by 2016Ra33.

& Band(A): Magnetic-dipole band 1. Magnetic-dipole rotational (shears) band based on 25/2$^-$ with proposed configuration=$\pi h^2_{11/2}\otimes\nu h^{-1}_{11/2}$ based on agreement of B(M1) values deduced from level lifetimes with the corresponding theoretical values.

a Band(B): Magnetic-dipole band 2. Possible magnetic-dipole rotational (shears) band based on 35/2$^-$ with tentative configuration=$\pi h^2_{11/2}\otimes\nu h^{-3}_{11/2}$ (theoretical calculation cannot reproduce experimental B(M1) and spin values simultaneously).

γ(^{141}Sm)

B(M1) values are in μ_N^2 units.

E$_\gamma$ †	I$_\gamma$	E$_i$(level)	J$_i^\pi$	E$_f$	J$_f^\pi$	Mult.#	δ@	α&	Comments
(1.58‡ *4*)		1.58	3/2$^+$	0.0	1/2$^+$				
(58.7‡)		3376.4	25/2$^-$	3317.8	(23/2$^-$)				E$_\gamma$: γ ray not observed in 2016Ra33 due to energy threshold restriction in Clover detectors.
100.2‡		2822.7	(23/2$^+$)	2722.4	(21/2$^+$)				
132.6 *1*	100.0	3509.0	27/2$^-$	3376.4	25/2$^-$	M1+E2	0.97 *28*	0.805 *20*	α(exp)=0.93 *18* DCO=1.31 *11* A$_2$=−0.19 *3*; A$_4$=−0.04 *1* B(M1)↓=2.92 *+55−48* δ: from DCO data. Others: 1.17 *+41−29* from $\gamma(\theta)$ data. α(exp): from transition intensity balance. R(ADO)=1.11 *7*. Recalculated for this evaluation: B(M1)=2.94 *98*.
174.2‡ *3*		175.8	11/2$^-$	1.58	3/2$^+$	M4			Mult.: from Adopted Gammas.
181.6‡		2822.7	(23/2$^+$)	2641.1	(23/2$^+$)				
222.5‡		2641.1	(23/2$^+$)	2418.6	(23/2$^-$)				
253.7 *1*	20.1 *28*	5594.3	37/2$^-$	5340.6	35/2$^-$	M1+E2	0.13 *8*	0.1260 *20*	DCO=0.72 *9* B(M1)↓=1.45 *+31−27* R(ADO)=0.84 *7*, POL=−0.23 *15*. Recalculated for this evaluation: B(M1)=1.62 *33*.
299.3 *3*	11.5 *18*	5940.0	39/2$^-$	5640.9	37/2$^-$	M1		0.0814	R(ADO)=0.66 *8*, POL=−0.13 *10*.
300.7 *3*	8.5 *12*	5640.9	37/2$^-$	5340.6	35/2$^-$	M1		0.0804	R(ADO)=0.75 *9*, POL=−0.15 *11*.
309.4 *1*	94.1 *51*	3818.4	29/2$^-$	3509.0	27/2$^-$	M1+E2	0.11 *7*	0.0742 *12*	DCO=0.68 *7* B(M1)↓=1.54 *+31−26* R(ADO)=0.63 *5*, POL=−0.13 *9*. Recalculated for this evaluation: B(M1)=1.68 *33*.
318.0 *3*	11.4 *19*	5640.9	37/2$^-$	5322.7	35/2$^-$	M1		0.0693	R(ADO)=0.78 *9*, POL=−0.21 *15*.
345.5 *3*	18.4 *21*	5940.0	39/2$^-$	5594.3	37/2$^-$	M1+E2	0.16 *7*	0.0553 *10*	DCO=0.75 *8* B(M1)↓>0.97 R(ADO)=0.81 *6*, POL=−0.12 *10*. Recalculated for this evaluation: B(M1)>0.66.
446.4 *1*	63.3 *41*	4264.8	31/2$^-$	3818.4	29/2$^-$	M1+E2	0.18 *8*	0.0284 *6*	DCO=0.77 *10* B(M1)↓=0.75 *+16−14* R(ADO)=0.70 *5*, POL=−0.22 *11*. Recalculated for this evaluation: B(M1)=0.84 *16*.
473.0 *3*	18.3 *35*	6413.0	41/2$^{(-)}$	5940.0	39/2$^-$	(M1)		0.0248	R(ADO)=0.89 *10*.
481.4 *3*	16.6 *27*	6894.4	43/2$^{(-)}$	6413.0	41/2$^{(-)}$	(M1)		0.0237	R(ADO)=0.92 *9*.
490.0 *3*	11.2 *21*	7384.4	45/2$^{(-)}$	6894.4	43/2$^{(-)}$	(M1)		0.0227	R(ADO)=0.79 *12*.

γ(^{141}Sm) (continued)

E_γ[†]	I_γ	E_i(level)	J_i^π	E_f	J_f^π	Mult.[#]	δ[@]	α[&]	Comments
519.2[‡]		2418.6	(23/2$^-$)	1899.4	(19/2$^-$)				
527.8 *1*	49.7 *54*	4792.6	33/2$^-$	4264.8	31/2$^-$	M1+E2	0.22 *9*	0.0184 *4*	DCO=0.81 *10* B(M1)↓=0.29 *+6−4* R(ADO)=0.69 *6*, POL=−0.23 *16*. Recalculated for this evaluation: B(M1)=0.33 *6*.
530.0 *3*	12.6 *19*	5322.7	35/2$^-$	4792.6	33/2$^-$	M1		0.0186	R(ADO)=0.52 *4*, POL=−0.18 *14*.
548.0 *1*	28.4 *40*	5340.6	35/2$^-$	4792.6	33/2$^-$	M1+E2	0.20 *7*	0.0168 *4*	DCO=0.79 *8* R(ADO)=0.84 *9*, POL=−0.19 *12*.
553.6[‡]		3376.4	25/2$^-$	2822.7	(23/2$^+$)				
573.0 *3*	6.8 *18*	5365.6	(35/2$^-$)	4792.6	33/2$^-$				
595.5[‡]		3317.8	(23/2$^-$)	2722.4	(21/2$^+$)				
634.8[‡]		810.6	15/2$^-$	175.8	11/2$^-$				
823.1[‡]		2722.4	(21/2$^+$)	1899.4	(19/2$^-$)				
1088.8[‡]		1899.4	(19/2$^-$)	810.6	15/2$^-$				
1418.3[‡]		3317.8	(23/2$^-$)	1899.4	(19/2$^-$)				

† Energy uncertainty is stated by 2016Ra33 as 0.1-0.3 keV, assigned as 0.1 keV for I$\gamma \geq 20$ and 0.3 keV for Iγ<20.

‡ From Adopted Levels, Gammas dataset of which many γ-rays were observed by 2016Ra33 (see spectra presented in Figs. 2 and 7 therein) but not included in the level scheme (Fig. 3).

From $\gamma\gamma(\theta)$(DCO), $\gamma\gamma(\theta)$(ADO), $\gamma\gamma$(linear polarization). Typical R(DCO) values for a stretched pure dipole (quadrupole) transition gated by a pure quadrupole (dipole) transition: 0.5 (2.0). Typical R(ADO) values for stretched dipole (quadrupole) transitions: 0.6 (1.6). Typical POL values: positive, negative, and near-zero numbers expected for transitions of electric, magnetic, and mixed character, respectively.

@ From DCO data using the alignment parameter σ/J=0.27, determined from pure ΔJ=1 E1 transitions in ^{143}Eu and ^{141}Sm.

& Total theoretical internal conversion coefficients, calculated using the BrIcc code (2008Ki07) with Frozen orbital approximation based on γ-ray energies, assigned multipolarities, and mixing ratios, unless otherwise specified.

$^{141}_{62}$Sm$_{79}$-3

$^{116}Cd(^{31}P,p5n\gamma)$ 2016Ra33

Level Scheme

Intensities: Relative I_γ

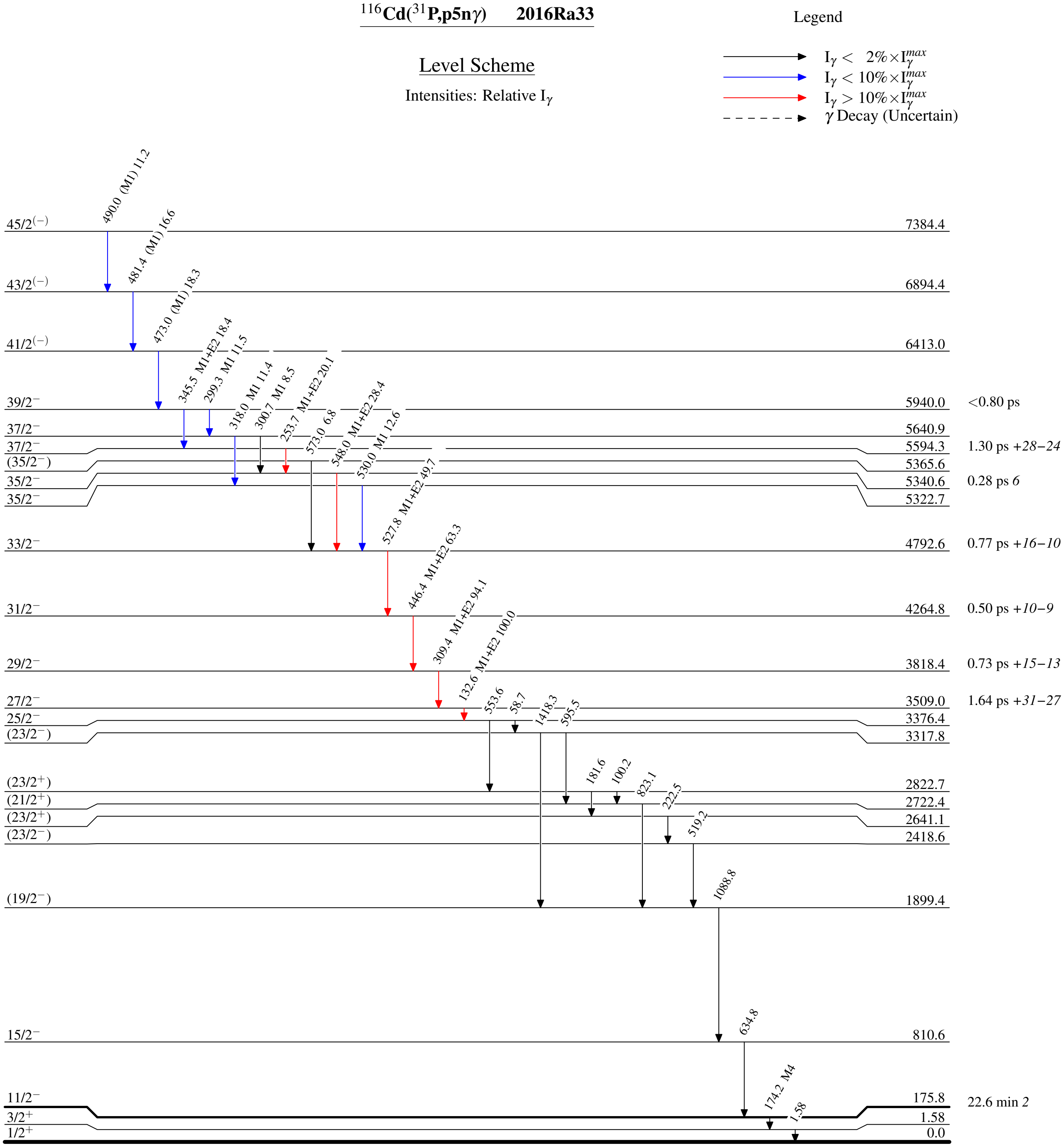

$^{141}_{62}Sm_{79}$

$^{116}Cd(^{31}P,p5n\gamma)$ 2016Ra33

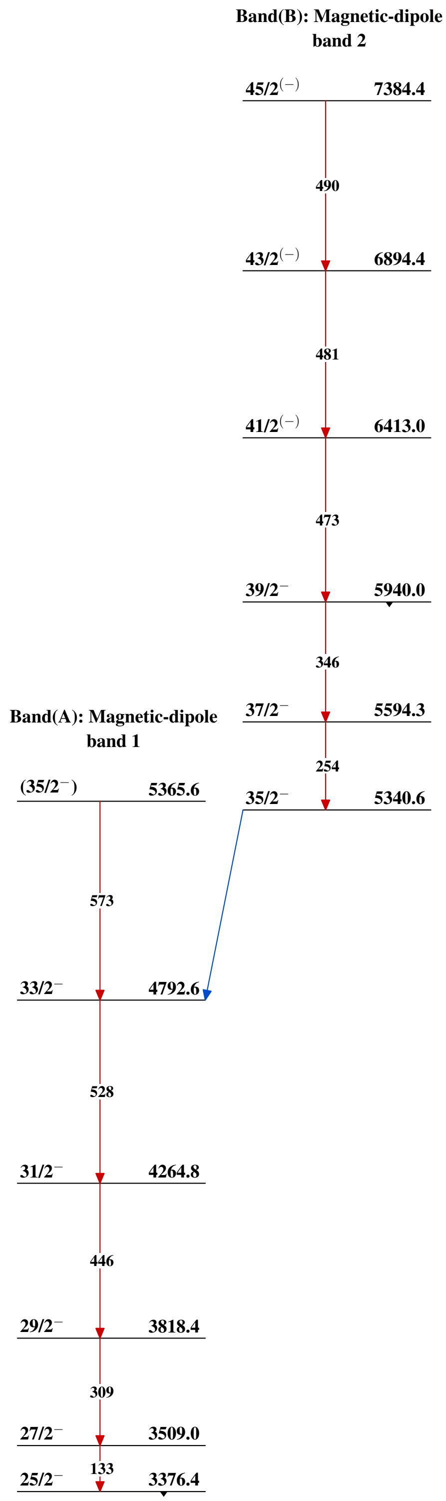

$^{141}_{62}Sm_{79}$